Contribution from the Departments of Chemistry and Mathematics, Washington State University, Pullman, Washington 99164-4630, and Department of Chemistry, Portland State University, Portland, Oregon 97207

Preparation and Crystal Structure of Dipyrazinium Trichromate and Bond Length Correlation for Chromate Anions of the Form $Cr_nO_{3n+1}^{2-}$

Mark R. Pressprich,[1a] Roger D. Willett,*[1a] R. D. Poshusta,[1a] Sam C. Saunders,[1b] Harry B. Davis,[1c] and Gary L. Gard[1c]

Received July 8, 1987

Pyrazine ($C_4H_4N_2$) reacts with chromium trioxide (CrO_3) in water to form dipyrazinium trichromate, $(C_4H_4N_2H)_2Cr_3O_{10}$. The deep red trichromate was obtained via recrystallization from water. Its crystal structure was determined by a single-crystal X-ray study. The crystals are monoclinic and belong to the space group $P2_1$ with $Z = 2$, $\beta = 91.44\ (2)°$, $a = 5.320\ (1)$ Å, $b = 10.613\ (3)$ Å, and $c = 13.743\ (4)$ Å at 23 (2) °C. The trichromate ion consists of three nearly tetrahedral CrO_4 groups joined through shared O atoms. The pyrazinium cations are linked to the trichromate anion through N-H···O hydrogen bonds. A comparison with crystallographic data on a series of mono- and polychromates shows a smooth correlation of the terminal and bridging Cr-O distances with increasing degree of polymerization. The correlation is done by means of a linear graphical plot and a graph theory cluster expansion.

Introduction

The preparation and reactions of high-valent chromium(VI) complexes continue to attract the attention of chemists who are interested in their ability to function as effective and selective oxidants. In previous studies we reported our results of using heterocyclic complexes and/or salts of high-valent chromium(VI) as new and selective oxidants with a number of primary and secondary alcohols in a nonaqueous system.[2,3] Using pyrazine ($C_4H_4N_2$), we reported the preparation of pyrazinium chlorochromate, $(C_4H_4N_2H)CrO_3Cl$, prepared from chromium trioxide, HCl(aq), and pyrazine.[2] If, however, one does not use HCl(aq) but only water, CrO_3, and pyrazine, an extremely interesting reaction occurs in which dipyrazinium trichromate is formed. Previous workers also have found that with organic bases it is possible to prepare chromates and polychromates, and they were able to obtain the first organic trichromate, $(Bu_4N)_2Cr_3O_{10}$, that could be recrystallized undecomposed from water.[4] We wish to report our results with pyrazine and chromium trioxide in water and in methylene chloride.

Experimental Section

Materials. Pyrazine ($C_4H_4N_2$) was obtained from Aldrich Chemical Co. and used as received. Chromium trioxide (CrO_3) was obtained from Baker Chemicals and prior to use was thoroughly dried under vacuum at 150°C for 4 h.

Preparation of $(C_4H_4N_2H)_2Cr_3O_{10}$. Into a 25-mL round-bottom Pyrex flask containing a Teflon-coated stirring bar were added 10.34 mmol of pyrazine and 306 mmol of H_2O. A second solution containing 10.03 mmol of CrO_3 and 55.6 mmol of H_2O at room temperature was added dropwise to the pyrazine solution. After approximately half of the CrO_3 solution was added and the mixture was stirred at 0 °C for 5 min, a large amount of solid formed. The remaining CrO_3 solution was then added dropwise, and the mixture was stirred for 15 min at 0 °C. After the solution stood for 1 h at 0 °C, deep orange crystals were collected on a sintered-glass funnel. The solid product was twice recrystallized from water, yielding a deep red solid that, when dried under vacuum for 16 h at room temperature, gave 1.50 mmol of $(C_4H_4N_2H)_2Cr_3O_{10}$ in 45% yield; mp 115.5 °C dec.

The infrared spectrum of the solid had the following bands (cm^{-1}): 3128 (mw), 3058 (mw), 1601 (w), 1586 (mw), 1488 (m), 1482 (m), 1472 (mw), 1367 (mw), 1168 (ms), 1109 (w), 1037 (w), 1017 (mw), 999 (w), 974 (ms), 965 (ms), 957 (s, sh), 947 (vs, sh), 938 (s), 916 (m), 900 (m), 887 (m), 859 (ms), 814 (vs, sh), 798 (s), 761 (s), 754 (ms), 723 (m), 650 (m), 600 (ms), 563 (mw), 515 (mw), 372 (ms). For the UV/vis spectrum (CH_3CN) the following peaks were found (nm): 382, 295 (sh), 269, 263, 256 (sh). Anal. Calcd for $C_8H_{10}N_4O_{10}Cr_3$: C, 20.09; H, 2.11; N, 11.72; Cr, 32.62. Found: C, 20.35; H, 2.13; N, 11.68; Cr, 33.19.

Table I. $(C_4H_4N_2H)_2Cr_3O_{10}$ Crystal Data

fw	478.18
a	5.320 (1) Å
b	10.613 (3) Å
c	13.743 (4) Å
β	91.44 (2)°
vol	775.7 (4) Å^3
cryst syst	monoclinic
space group	$P2_1$ (b axis unique)
Z	2
ρ(calcd)	2.05 g cm^{-3}
radiation[a]	Mo Kα
abs coeff	20.75 cm^{-1}
secondary extinction coeff[b]	0.005 21
transmission factors	0.762-0.964
temp	23 (2) °C
scan speed	4.0-29.3° min^{-1}
scan type	ω
scan range	1.8°
no. of stds monitored/no. of rflns	3/100
std rflns	002, 210, 111
rflns collected	1569
unique rflns	1449
unique rflns with $F_o > 3\sigma$	1434
weighting factor, g[c]	0.000 302
residual, $R(F)$[d]	0.0205
residual, $R_w(F)$[e]	0.0289
highest peak on final diff map	0.25 e/Å^3, 0.723 Å from C(1)
no. of params	227
final mean param shift/σ	0.012

[a] Graphite monochromated. [b] Defined so that $F_c^* = F_c/[1.0 + 0.002F^2/(\sin 2\theta)]^{0.25}$. [c] $w = 1/[\sigma^2(F) + gF^2]$. [d] $R = \sum||F_o| - |F_c||/\sum|F_o|$. [e] $R_w = [\sum w(|F_o| - |F_c|)^2/\sum w|F_o|^2]^{1/2}$.

Spectroscopic Equipment and Elemental Analyses. The infrared spectrum was recorded on a Perkin-Elmer 467 spectrophotometer. The UV-vis spectrum was taken by using a Cary 14 spectrophotometer. Elemental analyses were performed by Beller Mikroanalytisches Laboratorium, Göttingen, West Germany.

X-ray Crystallographic Measurements. A deep red, irregularly shaped (longest axis 0.6 mm) crystal of $(C_4H_4N_2H)Cr_3O_{10}$ suitable for single-crystal X-ray diffraction was selected with a polarizing microscope. The crystal was attached to a glass fiber with epoxy cement, and X-ray data were collected with a Nicolet R3m/E four-circle diffractometer using graphite-monochromated Mo Kα radiation. The crystal was determined to belong to Laue group $2/m$, and one-fourth of the sphere of reflection ($h,k \geq 0$,all l) was collected by using an ω-scan technique over a range of 3-50° in 2θ. Reflection intensities were standardized to allow for crystal degradation with 3 standard reflections collected every 100 reflections. No significant degradation was observed. Accurate unit cell parameters

(1) (a) Department of Chemistry, Washington State University. (b) Department of Mathematics, Washington State University. (c) Portland State University.
(2) Davis, H. B.; Sheets, R. M.; Brannfors, J. M.; Paudler, W. W.; Gard, G. L. *Heterocycles* **1983**, *20*, 2029.
(3) Davis, H. B.; Sheets, R. M.; Paudler, W. W.; Gard, G. L. *Heterocycles* **1984**, *22*, 2029.
(4) Behr, W. J.; Fuchs, J. *Z. Naturforsch., B: Anorg. Chem., Org. Chem.* **1975**, *30B*, 299.

0020-1669/88/1327-0260$01.50/0

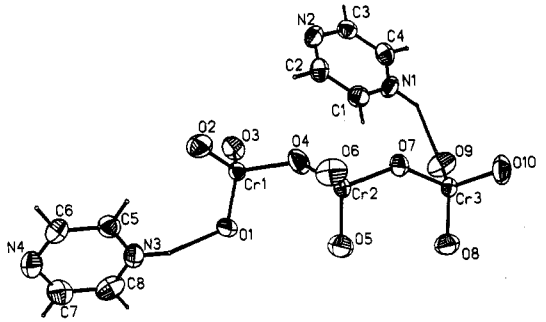

Figure 1. Thermal ellipsoid view of $(C_4H_4N_2H)_2Cr_3O_{10}$ at 50% probability including the shortest N–H···O hydrogen bonds. Hydrogen atom positions are indicated by small spheres.

were obtained through centering of 25 reflections with 2θ values between 31 and 33°. Pertinent crystallographic parameters are included in Table I.

The crystal structure was solved and refined with Nicolet SHELXTL, version 4.1 (1983), programs. Empirical absorption corrections were made by fitting the irregularly shaped crystal with a pseudoellipsoid refined from Ψ-scan data consisting of 5 reflections collected repetitively at 18 different orientations per reflection. The direct-methods program SOLV yielded most non-hydrogen atomic positions, and subsequent refinement was uneventful. The noncentric space group $P2_1$ was chosen over $P2_1/m$ from a tabulation of $\langle|E^2-1|\rangle$ (E's are normalized structure factors) versus $(\sin\theta)/\lambda$ thin-shell data, which yielded values closer to the theoretical limit of 0.736 (noncentric) than 0.968 (centric) for all 2θ. In order to define the origin for this space group, the y coordinate of Cr(1) was fixed. All atoms (including hydrogen) were located by unsharpened Fourier difference techniques. As it is ambiguous which nitrogen atom of the pyrazine ions is protonated, the location of hydrogen atoms by difference techniques was of significant value. Specifically, hydrogen atoms were located near N(1) and N(3) and not by N(2) or N(4) (see Figure 1). All non-hydrogen atoms were refined anisotropically with the SHELXTL blocked-cascade least-squares refinement program. Hydrogen atom positions were fixed positionally at C–H and N–H equal to 0.96 Å, and isotropic thermal parameters were fixed at values approximately 1.2 times larger than the equivalent isotropic thermal parameters of the corresponding heavier atoms. An attempt was made to allow hydrogen atom positions to be refined independently, but this led to poor convergence of parameter mean shift per σ and a marginal overdeterminancy of observed reflections to total parameters of 5.6. With constrained hydrogen atoms, refinement of all 227 parameters reached convergence with a final parameter mean shift per σ of 0.012. Minimization of the weighted residual R_w led to final discrepancy indices of $R_w(F) = 0.029$ and $R(F) = 0.021$. Anomalous scattering effects allowed an absolute configuration determination for this polar space group. In a left-handed coordinate system the structure was refined with $R_w(F) = 0.035$ ($R(F) = 0.023$). Thus, the structure belongs to $P2_1$ with right-handed axes. Positional parameters and equivalent isotropic thermal parameters are listed in Table II. Table III gives pertinent bond distances and angles.

Results and Discussion

In previous studies[2] with pyrazine, it was found that with CrO_3 in HCl(aq) pyrazinium chlorochromate, $(C_4H_4N_2H)CrO_3Cl$, was formed; without water and HCl(aq) but in the presence of a nonaqueous system, a different product was obtained:[3]

$$C_4H_4N_2 + CrO_3 \xrightarrow{CH_2Cl_2} C_4H_4N_2{\cdot}CrO_3 \qquad (1)$$

This bright yellow solid is stable when shielded from light and kept under a nitrogen atmosphere; no melting was observed upon heating to 350 °C. The infrared spectrum of the $C_4H_4N_2{\cdot}CrO_3$ complex contains bands at 928 and 902 cm^{-1} that are attributable to the ν_{as} and ν_s Cr–O stretch.[3] The assignment of the absorption bands in the 280–312-cm^{-1} region is assigned to the Cr–N vibrational modes[3] and is similar to assignments made for the $MoOCl_3{\cdot}C_4H_4N_2$ complex[5] as well as the assignment of the 285–290-cm^{-1} infrared absorptions in various Etard complexes.[6] It is thought that, in $C_4H_4N_2{\cdot}CrO_3$, the pyrazine is acting as a bridging bidentate ligand and the complex is polymeric. The failure of the complex to melt and its general insolubility supports this idea. Confirmation of this structure must await the preparation of suitable crystals for X-ray study. By comparison, the infrared and UV/vis spectra of pyrazinium chlorochromate supports a structure composed of pyrazinium and chlorochromate ions.[2]

In an interesting reaction, chromium trioxide in water reacts with pyrazine at 0 °C to give dipyrazinium trichromate:

$$2C_4H_4N_2 + 3CrO_3 + H_2O \rightarrow (C_4H_4N_2H)_2Cr_3O_{10} \qquad (2)$$

(5) Carmichael, W. M.; Edwards, D. A. *J. Inorg. Nucl. Chem.* **1970**, *32*, 1199.
(6) Makhija, R. C.; Stairs, R. A. *Can. J. Chem.* **1968**, *46*, 1255.

Table II. Non-Hydrogen Atomic Coordinates and Isotropic Thermal Parameters (Å²) for $(C_4H_4N_2H)_2Cr_3O_{10}$

atom	x	y	z	U_{iso}[a]
Cr(1)	0.1164 (1)	1.0000[b]	0.7592 (1)	0.026 (1)
Cr(2)	0.2119 (1)	1.2956 (1)	0.8209 (1)	0.025 (1)
Cr(3)	0.2388 (1)	1.5419 (1)	0.6764 (1)	0.026 (1)
O(1)	0.4131 (4)	0.9667 (3)	0.7653 (2)	0.036 (1)
O(2)	−0.0231 (5)	0.9383 (3)	0.8489 (2)	0.049 (1)
O(3)	−0.0065 (5)	0.9542 (3)	0.6579 (2)	0.044 (1)
O(4)	0.0760 (5)	1.1691 (3)	0.7620 (2)	0.051 (1)
O(5)	0.5066 (5)	1.2847 (3)	0.8196 (2)	0.045 (1)
O(6)	0.1277 (5)	1.2998 (4)	0.9303 (2)	0.049 (1)
O(7)	0.1125 (4)	1.4301 (3)	0.7622 (2)	0.040 (1)
O(8)	0.5364 (4)	1.5310 (3)	0.6788 (2)	0.046 (1)
O(9)	0.1245 (5)	1.5093 (4)	0.5701 (2)	0.051 (1)
O(10)	0.1527 (6)	1.6803 (3)	0.7092 (2)	0.052 (1)
N(1)	0.3165 (6)	−0.1362 (3)	0.4956 (2)	0.038 (1)
N(2)	0.6121 (6)	−0.3398 (3)	0.4611 (2)	0.040 (1)
N(3)	0.4730 (6)	0.2643 (3)	0.1127 (2)	0.037 (1)
N(4)	0.4575 (6)	0.0368 (4)	0.0226 (2)	0.046 (1)
C(1)	0.2637 (7)	−0.2095 (4)	0.4193 (3)	0.040 (1)
C(2)	0.4146 (7)	−0.3120 (4)	0.4043 (3)	0.039 (1)
C(3)	0.6594 (7)	−0.2626 (4)	0.5365 (3)	0.037 (1)
C(4)	0.5121 (7)	−0.1591 (4)	0.5551 (3)	0.039 (1)
C(5)	0.6368 (7)	0.2372 (4)	0.0454 (3)	0.037 (1)
C(6)	0.6259 (7)	0.1220 (4)	0.0022 (3)	0.040 (1)
C(7)	0.2969 (7)	0.0678 (4)	0.0914 (3)	0.050 (1)
C(8)	0.3025 (7)	0.1813 (5)	0.1385 (3)	0.047 (1)

[a] Equivalent isotropic U defined as one-third of the trace of the orthogonalized U_{ij} tensor. [b] Fixed coordinate.

Table III. Non-Hydrogen Bond Lengths (Å) and Angles (deg) for $(C_4N_2H_5)_2Cr_3O_{10}$

	Trichromate Anion		
Cr(1)–O(1)	1.618 (2)	Cr(2)–O(6)	1.580 (2)
Cr(1)–O(2)	1.596 (3)	Cr(2)–O(7)	1.716 (3)
Cr(1)–O(3)	1.599 (3)	Cr(3)–O(7)	1.814 (3)
Cr(1)–O(4)	1.808 (3)	Cr(3)–O(8)	1.587 (2)
Cr(2)–O(4)	1.718 (3)	Cr(3)–O(9)	1.605 (3)
Cr(2)–O(5)	1.573 (3)	Cr(3)–O(10)	1.606 (3)
O(1)–Cr(1)–O(2)	110.0 (1)	O(5)–Cr(2)–O(6)	108.6 (1)
O(1)–Cr(1)–O(3)	110.9 (1)	O(5)–Cr(2)–O(7)	110.6 (1)
O(1)–Cr(1)–O(4)	109.4 (1)	O(6)–Cr(2)–O(7)	109.4 (2)
O(2)–Cr(1)–O(3)	111.1 (1)	Cr(2)–O(7)–Cr(3)	137.3 (1)
O(2)–Cr(1)–O(4)	109.4 (2)	O(7)–Cr(3)–O(8)	108.9 (1)
O(3)–Cr(1)–O(4)	105.9 (1)	O(7)–Cr(3)–O(9)	108.2 (1)
Cr(1)–O(4)–Cr(2)	137.5 (2)	O(7)–Cr(3)–O(10)	107.6 (1)
O(4)–Cr(2)–O(5)	110.2 (2)	O(8)–Cr(3)–O(9)	111.0 (1)
O(4)–Cr(2)–O(6)	110.1 (2)	O(8)–Cr(3)–O(10)	110.6 (2)
O(4)–Cr(2)–O(7)	107.9 (1)	O(9)–Cr(3)–O(10)	110.4 (2)
	Pyrazinium Cations		
N(1)–C(1)	1.329 (5)	N(3)–C(5)	1.318 (5)
N(1)–C(4)	1.330 (5)	N(3)–C(8)	1.319 (5)
C(1)–C(2)	1.371 (6)	C(5)–C(6)	1.360 (6)
N(2)–C(2)	1.327 (5)	N(4)–C(6)	1.309 (5)
N(2)–C(3)	1.339 (5)	N(4)–C(7)	1.331 (5)
C(3)–C(4)	1.377 (6)	C(7)–C(8)	1.367 (6)
N(1)–C(1)–C(2)	118.1 (3)	N(3)–C(5)–C(6)	118.7 (4)
C(1)–C(2)–N(2)	123.1 (4)	C(5)–C(6)–N(4)	123.3 (4)
C(2)–N(2)–C(3)	116.8 (3)	C(6)–N(4)–C(7)	115.9 (4)
N(2)–C(3)–C(4)	122.3 (3)	N(4)–C(7)–C(8)	123.1 (4)
C(3)–C(4)–N(1)	118.1 (3)	C(7)–C(8)–N(3)	118.0 (4)
C(4)–N(1)–C(1)	121.6 (3)	C(8)–N(3)–C(5)	120.9 (4)

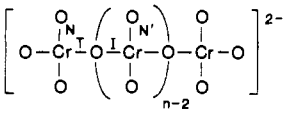

Figure 2. Classification of Cr–O bonds within $Cr_nO_{3n+1}^{2-}$ anions. N and N′ represent nonbridging Cr–O bonds (O connected to terminal and interior Cr, respectively), T represents terminal bridging Cr–O bonds, and I represents inner bridging Cr–O bonds.

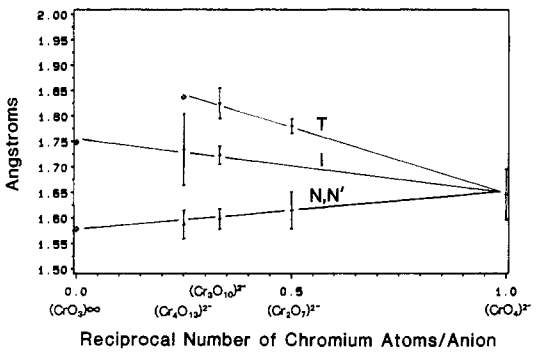

Figure 3. Correlation of Cr–O bond types (see Figure 2) within $Cr_nO_{3n+1}^{2-}$ anions ($\pm 2\sigma$ confidence limits).

It is thought that the first product formed under these conditions is $(C_4H_4N_2H)_2Cr_2O_7$ but that the dichromate reacts further with an additional 1 mol of CrO_3 to produce the trichromate. For example, rubidium trichromate has been prepared from its dichromate with excess CrO_3.[7] Dipyrazinium trichromate is a deep red solid that melts with decomposition at 115.5 °C.

The infrared spectrum of dipyrazinium trichromate contains the expected C–H vibrations. In the 900–976-cm^{-1} region strong symmetric and asymmetric Cr–O stretching bands are found and are similar to those reported for $Cs_2Cr_3O_{10}$.[8] The infrared spectrum indicates that this complex is composed of polychromate groups, the trichromate group being favored.

While it is possible to suggest that the pyrazinium complex, prepared in water, is a trichromate, it was necessary to carry out a crystal structure for exact determination. Figure 1 shows the crystal structure of dipyrazinium trichromate consisting of $C_4H_5N_2^+$ and $Cr_3O_{10}^{2-}$ ions. The trichromate ion is composed of three corner-sharing tetrahedra. The shortest hydrogen-bonding distances between the trichromate anion and the two pyrazinium cations are O(9)–H(1A) = 2.205 Å and O(1)–H(3A) = 1.877 Å. The corresponding O–N distances are O(9)–N(1) = 2.933 Å and O(1)–N(3) = 2.781 Å. Cr–O distances of the trichromate ion show no substantial deviations from previously studied trichromate structures.[7,9-11] Distances vary from 1.573 (3) to 1.618 (2) Å for nonbridging Cr–O bonds and from 1.807 (3) to 1.814 (3) Å for terminal bridging Cr–O bonds. Nonbridging bond angles are nearly tetrahedral, 105.9 (1)–111.1 (2)°, with bridging bond angles of 137.3 (1)–137.5 (2)°. Non-hydrogen bond lengths and angles for the complex are shown in Table III.

By classifying the Cr–O bonds according to the scheme shown in Figure 2, one can make an interesting comparison of Cr–O bond lengths for all types of chromates of the form $Cr_nO_{3n+1}^{2-}$. From this classification, Figure 3 and Table IV show a comparison of 12 monochromates (CrO_4^{2-}),[12-23] 15 dichromates ($Cr_2O_7^{2-}$),[24-31] 4 trichromates ($Cr_3O_{10}^{3-}$)[7,9,10] (including dipyrazinium trichromate), 1 tetrachromate ($Cr_4O_{13}^{2-}$),[24] and the polychromate

Table IV

Mean Cr–O Bond Lengths (Å)

bond type[a]	CrO_4^{2-}	$Cr_2O_7^{2-}$	$Cr_3O_{10}^{2-}$	$Cr_4O_{13}^{2-}$	$(CrO_3)_\infty$
N, N′ bonds	1.646 (25)	1.615 (18)	1.598 (10)	1.587 (14)	1.578 (–)
I bonds			1.723 (9)	1.734 (35)	1.748 (–)
T bonds		1.780 (7)	1.825 (15)	1.837 (–)	

Chromate Structures Analyzed in This Study

chromate	ref
Monochromates	
$(NH_4)_2CrO_4$	12
$(NH_4)_2Ni(CrO_4)_2 \cdot 6H_2O$	13
$Ce(CrO_4)_2 \cdot 2H_2O$	14
$[Co(NH_3)_6](CrO_4)Cl \cdot 3H_2O$	15
$UO_2CrO_4 \cdot 5.5H_2O$	16
Li_2CrO_4	17
$CaCrO_4 \cdot H_2O$	18
$HgCrO_4$	19
$Fe(CrO_4)_3 \cdot 3H_2O$ (α form)	20
K_2CrO_4 (α form)	21
$NaCrO_4 \cdot 4H_2O$	22
$(CN_3H_6)_2CrO_4$	23
Dichromates	
$Na_2Cr_2O_7$ ($P\bar{1}$ form)	24
$Na_2Cr_2O_7$ ($A\bar{1}$ form)	24
$K_2Cr_2O_7$ ($P\bar{1}$ form)	24
$Rb_2Cr_2O_7$ ($P\bar{1}$ form)	24
$Rb_2Cr_2O_7$ ($P2_1/n$ form)	24
$Rb_2Cr_2O_7$ ($C2/c$ form)	24
$NaRbCr_2O_7$	24
$CdK_2(Cr_2O_7)_2 \cdot 2H_2O$	25
$Ag_2Cr_2O_7$	26
$HgCl_2 \cdot K_2Cr_2O_7$	27
$HgCl_2 \cdot (NH_4)_2Cr_2O_7$	27
$Cd(NH_4)_2(Cr_2O_7)_2 \cdot 2H_2O$	28
$(NH_4)_2Cr_2O_7$	29
$CuCr_2O_7 \cdot 2H_2O$	30
$BaCr_2O_7$ (α form)	31
Trichromates	
$(NH_4)_2Cr_3O_{10}$	9
$K_2CrO_3O_{10}$	10
$Rb_2Cr_3O_{10}$	7
$(C_4H_4N_2H)_2Cr_3O_{10}$	this study
Tetrachromate	
$Rb_2Cr_4O_{13}$	24
Polychromate	
$(CrO_3)_\infty$	32

[a] N, N′, I, and T type bonds are defined in Figure 2 and in the text. Variabilities for the N, N′, I, and T type Cr–O bonds correspond to ±1 estimated standard deviation from a weighted mean bond length for each bond type. Note that the variabilities do not correspond to experimental error (see the Appendix). Data were collected from all types of chromates (e.g. six N values per dichromate anion) weighted so that an equal amount of data were collected from each structure. No variabilities are specified for some of the bond types due to minimal data (e.g. two crystallographically obtained N bond lengths for $(CrO_3)_\infty$). For the same reason, variabilities for $Cr_4O_{13}^{2-}$ should probably be viewed skeptically since only one tetrachromate structure was analyzed.

(7) Löfgren, P. *Chem. Scr.* **1974**, *5*, 91.
(8) Mattes, R. *Z. Anorg. Allg. Chem.* **1971**, *382*, 163.
(9) Blum, P. D.; Guitel, J. C. *Acta Crystallogr., Sect. B: Struct. Crystallogr. Cryst. Chem.* **1980**, *B36*, 135.
(10) Blum, P. D.; Averbuch-Pouchot, M. T.; Guitel, J. C. *Acta Crystallogr., Sect. B: Struct. Crystallogr. Cryst. Chem.* **1979**, *B35*, 454.
(11) Stępień, A.; Grabowski, M. J. *Acta Crystallogr., Sect. B: Struct. Crystallogr. Cryst. Chem.* **1977**, *B33*, 2924.
(12) Stephens, J. S.; Cruickshank, D. W. J. *Acta Crystallogr., Sect. B: Struct. Crystallogr. Cryst. Chem.* **1970**, *B26*, 437.
(13) Montgomery, H. *Acta Crystallogr., Sect. B: Struct. Crystallogr. Cryst. Chem.* **1979**, *B35*, 155.
(14) Lindgren, O. *Acta Chem. Scand. Ser. A* **1977**, *A31*, 167.
(15) Figgis, B. N.; Skelton, B. W.; White, A. H. *Aust. J. Chem.* **1979**, *32*, 417.
(16) Serezhkin, V. N.; Trunov, V. K. *Sov. Phys.—Crystallogr. (Engl. Transl.)* **1981**, *26*(2), 169.
(17) Brown, I. D.; Faggiani, R. *Acta Crystallogr., Sect. B: Struct. Crystallogr. Cryst. Chem.* **1975**, *B31*, 2364.
(18) Bars, P. O.; Le Marouille, J. Y.; Grandjean, D. *Acta Crystallogr., Sect. B: Struct. Crystallogr. Cryst. Chem.* **1977**, *B33*, 3751.
(19) Stålhandske, C. *Acta Crystallogr., Sect. B: Struct. Crystallogr. Cryst. Chem.* **1978**, *B34*, 1968.

Table V. Irreducible Cluster Contributions to Cr–O Bond Lengths (Å)

	γ			
	•	•–•	•–•–•	•–•–•–•
$l_{N,N'}(\gamma)$	1.646 (25)	−1.677 (53)	0.014 (45)	0.006 (30)
$l_T(\gamma)$	1.646 (25)	−1.512 (51)	−0.089 (33)	−0.033 (−)
$l_I(\gamma)$	1.646 (25)	−1.512 (51)	−0.191 (30)	−0.068 (−)
$l'_{N,N'}(\gamma)$	0.000 (25)	−0.031 (53)	0.014 (45)	0.006 (30)
$l'_T(\gamma)$	0.000 (25)	0.134 (51)	−0.089 (33)	−0.033 (−)
$l'_I(\gamma)$	0.000 (25)	0.134 (51)	−0.191 (30)	−0.068 (−)

$(CrO_3)_\infty$.[32] The chromates selected for this structural comparison follow the criteria of Löfgren:[24] only structures that have been studied by single-crystal X-ray diffraction with estimated standard deviations in the Cr–O distances of $\sigma < 0.02$ Å are included. All bond distances in this comparison are uncorrected for thermal motion. Figure 3 shows several general trends for the various types of Cr–O bonds. Terminal bridging bond lengths (T type bonds) and inner tetrahedral bridging bond lengths (I type bonds) increase smoothly on average in correlation with increasing polymerization of the chromates. Similarly, nonbridging bond lengths (N type bonds) show an equally smooth decrease in Cr–O bond length on average with increasing polymerization. Note that one might distinguish N from N′ type nonbridging bonds in correlating chromate bond lengths, where the two subtypes may be classified according to whether the nonbridging oxygen is bonded to a terminal chromium atom (N type bond) or an interior chromium atom (N′ type bond). N′ type bonds appear to be shorter on average than N type bonds, but only the tri- and tetrachromates have both bond types, and consequently there is not yet enough empirical data to justify this distinction.

Cr–O bond lengths may also be examined in terms of a cluster expansion:[33]

$$L(\Gamma) = \sum_{\gamma \in \Gamma} N(\Gamma,\gamma)\, l(\gamma) \qquad (3)$$

A graph-theoretical notation is used here: Γ is the graphical symbol for the $Cr_nO_{3n+1}^{2-}$ moiety. Then $L(\Gamma)$ is the length of Cr–O bonds (N, N′, I, or T) in this structure. Similarly, γ is a subgraph of Γ representing a cluster within $Cr_nO_{3n+1}^{2-}$. For example, $Cr_3O_{10}^{2-}$ is abbreviated by the graph •–•–• (oxygen atoms are suppressed; each vertex corresponds to a Cr atom). There are three clusters CrO_3 (•) and two clusters Cr_2O_6 (•–•) within $Cr_3O_{10}^{2-}$. The summation extends over all connected subgraphs within Γ (including Γ itself). The coefficient $N(\Gamma,\gamma)$ is the number of times the subgraph γ is embedded within Γ: $N(\bullet\text{–}\bullet\text{–}\bullet,\bullet) = 3$, $N(\bullet\text{–}\bullet\text{–}\bullet,\bullet\text{–}\bullet) = 2$, $N(\bullet\text{–}\bullet\text{–}\bullet\text{–}\bullet,\bullet\text{–}\bullet\text{–}\bullet) = 1$, etc.

This cluster expansion resembles Mayer's cluster expansion in statistical mechanics.[34] It may be used to interpret and quantify the intuitive belief that bond lengths are smooth functions of molecular structure. In this case, structure is expressed in the relation between vertices of the graph: either they are connected by an edge or they are not. The bond length ($L(\Gamma)$ receives contributions from the totality of the graph as resolved into all possible subgraphs. Thus, $l(\gamma)$ is the (irreducible) cluster contribution made to L by each subgraph γ that appears in Γ. Formula 3 can be used for properties other than bond lengths to find irreducible contributions of various clusters to these properties.[33]

Given $L(\Gamma)$ for Γ = •, •–•, •–•–•, etc., the cluster expansion may be easily inverted to yield the irreducible cluster contributions, $l(\gamma)$. Also, the variabilities in $L(\gamma)$ propagate through the inversion formulas to give variabilities for $l(\gamma)$. These values of $l(\gamma)$ and their associated estimated 1σ deviations are shown in Table V for Cr–O bond lengths of each type in $Cr_nO_{3n+1}^{2-}$ for N = 1–4. Here we have taken $L_I(\bullet) = L_T(\bullet) = L_{N,N'}(\bullet)$ and $L_I(\bullet\text{–}\bullet) = L_T(\bullet\text{–}\bullet)$.

Another approach is to choose the reference Cr–O bond length to be 1.646 Å and only perform the cluster expansion on the departure from this bond length:

$$L(\Gamma) - 1.616 = \sum_{\gamma \in \Gamma} N(\Gamma,\gamma)\, l'(\gamma) \qquad (4)$$

Values of l' are also tabulated in Table V.

Conclusions about the irreducible cluster contributions must be tempered by their large calculated variabilities. However, it appears that convergence is reasonably rapid, and the influence of neighboring CrO_3 groups decreases with distance in agreement with intuition. Convergence is evident in the trend of $l(\gamma)$ approaching zero as γ becomes large. That is, the influence of remote CrO_3 groups is weaker than nearby groups. Variability in irreducible cluster contributions to bond lengths is larger than that in the lengths themselves. This is because $l(\gamma)$ accumulates variability from as many as three $L(\Gamma)$ values in the inversion formula. Even if the estimated 1σ deviation in $L(\Gamma)$ were only 0.001 Å, the estimated 1σ deviation in $l(\gamma)$ would still be approximately 0.002 Å (still 30% relative error in $l(\bullet\text{–}\bullet\text{–}\bullet\text{–}\bullet)$).

Preliminary calculations show that another useful correlation for the chromate anions might be made. As has been previously noted for the alkali-metal chromates,[24] while there are wide variations of bond lengths within individual tetrahedra, the mean Cr–O bond length per tetrahedron for all chromates appears to be fairly independent of molecular environment, as one intuitively expects from simple electrostatic considerations. To clarify this point, one might imagine that as one of the four tetrahedral Cr–O bonds is lengthened the other three Cr–O bonds will correspondingly shorten so that the overall Cr–O bond length average per tetrahedron remains approximately constant (~1.616 Å). This conclusion must remain tentative until a satisfactory statistical model can be developed (see the Appendix).

A similar empirical examination of bond lengths in other polymeric complexes might also be informative. The validity of this correlation depends on consistency in bond angles, however, and so a comparison of, for example, chlorocuprates with their widely varying geometries will be more difficult than a comparison of compounds with rigid monomeric units.[35,36]

Acknowledgment. H.B.D. and G.L.G. acknowledge gratefully the support of the donors of the Petroleum Research Fund, administered by the American Chemical Society. The X-ray diffraction facility was established through funds from the National Science Foundation (Grant No. CHE-840840), the Boeing Corp., and Washington State University.

Appendix: Statistical Analysis

The statistical analysis of the confluence of the sources of variation in this problem is not ordinary and requires the examination of a special mathematical model. Consideration must be made for the two sources of variation inherent to the study of bond lengths of one bond type: N, N′; T; I. The first is the ineradicable

(20) Riou, P. A.; Bonnin, A. *Acta Crystallogr., Sect. B: Struct. Crystallogr. Cryst. Chem.* **1978**, *B34*, 706.
(21) Toriumi, K.; Saito, Y. *Acta Crystallogr., Sect. B: Struct. Crystallogr. Cryst. Chem.* **1978**, *B34*, 3149.
(22) Ruben, H.; Olovsson, I.; Zalkin, A.; Templeton, D. H. *Acta Crystallogr., Sect. B: Struct. Crystallogr. Cryst. Chem.* **1973**, *B29*, 2963.
(23) Cygler, M.; Grabowski, M. J.; Stępień, A.; Wajsman, E. *Acta Crystallogr., Sect. B: Struct. Crystallogr. Cryst. Chem.* **1976**, *B32*, 2391.
(24) Löfgren, P. *Chem. Commun., Univ. Stockholm* **1974**, *No. 5* and references therein.
(25) Durif, P. A.; Averbuch-Pouchot, M. T. *Acta Crystallogr., Sect. B: Struct. Crystallogr. Cryst. Chem.* **1979**, *B35*, 1456.
(26) Durif, P. A.; Averbuch-Pouchot, M. T. *Acta Crystallogr., Sect. B: Struct. Crystallogr. Cryst. Chem.* **1978**, *B34*, 3335.
(27) Averbuch-Pouchot, M. T.; El-Horr, N.; Guitel, J. C. *Acta Crystallogr., Sect. C: Cryst. Struct. Commun.* **1984**, *C40*, 725.
(28) Blum, P. D.; Durif, A.; Guitel, J. C. *Acta Crystallogr., Sect. B: Struct. Crystallogr. Cryst. Chem.* **1980**, *B36*, 137.
(29) Dalgaard, G.A.P.; Hazell, A. C.; Hazell, R. G. *Acta Chem. Scand., Ser. A* **1974**, *A28*, 541.
(30) Blum, P. D.; Suitel, J. C. *Acta Crystallogr., Sect. B: Struct. Crystallogr. Cryst. Chem.* **1980**, *B36*, 667.
(31) Blum, P. D.; Averbuch-Pouchot, M. T.; Guitel, J. C. *Acta Crystallogr., Sect. B: Struct. Crystallogr. Cryst. Chem.* **1979**, *B35*, 2685.
(32) Stephens, J. S.; Cruickshank, D. W. J. *Acta Crystallogr., Sect. B: Struct. Crystallogr. Cryst. Chem.* **1970**, *B26*, 222.
(33) Klein, D. J. *Int. J. Quantum Chem., Quantum Chem. Symp.* **1986**, *No. 20*, 153.
(34) Mayer, J. E. *J. Chem. Phys.* **1950**, *18*, 1476.
(35) Smith, D. W. *Coord. Chem. Rev.* **1976**, *21*, 93.
(36) Willett, R. D.; Geiser, U. *Croat. Chem. Acta* **1984**, *57*, 737.

experimental error in the measured bond length; the second is the variability of the true bond lengths themselves due to physical perturbations of the crystalline lattice, such as hydrogen bonding.

Suppose that a certain set of m bonds of one bond type have been selected for measurement. Let us fix our attention on the jth bond ($j = 1, ..., m$) and assume it to have a perturbed length y_j. Measurement of y_j will contain experimental error. We assume the errors are such that the measurement on the perturbed length is a conditional Gaussian (normal) variate with a known standard error σ_j, i.e.

$$X|y_j \approx N(y_j,\sigma_j^2) \tag{5}$$

that has density

$$f_{X|y_j}(x) = \frac{1}{(2\pi)^{1/2}\sigma_j}\exp\left\{-\frac{1}{2}\left(\frac{x-y_j}{\sigma_j}\right)^2\right\} \equiv \frac{1}{\sigma_j}\varphi\left(\frac{x-y_j}{\sigma_j}\right) \tag{6}$$

Here we adopt the standard statistical notation of upper-case letters for random variables and the corresponding lower-case letters for their observed values. The notation in (5) means simply that we have a normal population with mean y_j and variance σ_j^2; i.e., repeated measurement of a particular bond length, y_j, will yield a Gaussian distribution of values centered at y_j characterized by a standard error σ_j. φ denotes the standard normal density.

However, the m perturbed bond lengths y_j for $j = 1, ..., m$ also form a population that, from the noncontradictory evidence of sample histograms for N, N′ and for T bond types and the entailed mathematical simplicity, we also assume to be Gaussian with a mean value μ and a variance σ^2, i.e.

$$Y_j \approx N(\mu,\sigma^2) \qquad j = 1, ..., n \tag{7}$$

Both parameters μ and σ^2 are unknown, and their correct estimation from the data is the goal of this analysis. We recognize that the experimental data for a given bond type are a convolution of this distribution with the experimental errors associated with each measurement. From (5) and (7) and the calculus of probabilities we obtain the unconditional distribution of the observation for the jth perturbed bond length to be

$$X_j \approx N(\mu,\sigma_j^2 + \sigma^2) \qquad j = 1, ..., m \tag{8}$$

To obtain the *maximum likelihood estimates* of μ and σ^2, we maximize the likelihood function of the sample data from (8). We maximize

$$L(\mu,\sigma^2) = \prod_{j=1}^{m}\frac{1}{(\sigma_j^2 + \sigma^2)^{1/2}}\varphi\left[\frac{x_j - \mu}{(\sigma_j^2 + \sigma^2)^{1/2}}\right] \tag{9}$$

by setting

$$\frac{\partial L}{\partial \mu} = 0 \qquad \frac{\partial L}{\partial \sigma^2} = 0$$

and solving the coupled equations in μ and σ^2, namely

$$\mu = \sum_{j=1}^{m}\frac{x_j}{\sigma_j^2 + \sigma^2}\Big/\sum_{j=1}^{m}\frac{1}{\sigma_j^2 + \sigma^2} \tag{10}$$

and

$$\sum_{j=1}^{m}\frac{1}{\sigma_j^2 + \sigma^2} = \sum_{j=1}^{m}\frac{(x_j - \mu)^2}{(\sigma_j^2 + \sigma^2)^2} \tag{11}$$

Equations 10 and 11 were solved via a computer program to give the estimated 1σ deviation from the mean μ for the various bond types, exhibited in Table IV and Figure 3.

Registry No. $(C_4H_4N_2H)_2Cr_3O_{10}$, 111348-98-2.

Supplementary Material Available: Tables SI and SII, listing thermal parameters and derived hydrogen atom positions, and Figure SI, a diagram of the unit cell packing (3 pages); a table of calculated and observed structure factors (9 pages). Ordering information is given on any current masthead page.

Contribution from the Department of Chemistry 6-331, Massachusetts Institute of Technology, Cambridge, Massachusetts 02139

Synthesis and Reactivity of Two Monomeric Tungsten(IV) Phenoxide Complexes

Mark L. Listemann, Richard R. Schrock,* John C. Dewan, and Richard M. Kolodziej

Received July 8, 1987

$W(DIPP)_4$ (DIPP = O-2,6-C_6H_3-*i*-Pr_2) has been prepared by adding LiDIPP to $WCl_4(Et_2S)_2$. $W(DMP)_4$ (DMP = O-2,6-$C_6H_3Me_2$) can be prepared by an analogous procedure or by reducing *trans*-$W(DMP)_4Cl_2$ with sodium in ether. $W(DIPP)_4$ belongs to the space group $C2/c$ with a = 30.557 (5) Å, b = 13.434 (2) Å, c = 23.312 (3) Å, β = 91.99 (1)°, V = 9153.6 Å^3, and Z = 8. Final R_1 = 0.042 and R_2 = 0.046. $W(DIPP)_4$ contains a ruffled distorted square planar WO_4 core with trans O–W–O angles of 168°, cis O–W–O angles of 90–91°, and W–O–C angles of 154–159°. $W(DMP)_4$ belongs to the space group $P4/n$ with a = b = 14.475 (2) Å, c = 7.097 (3) Å, V = 1487.0 Å^3, and Z = 2. Final R_1 = 0.055 and R_2 = 0.057. $W(DMP)_4$ contains an essentially planar WO_4 core in which trans O–W–O angles are 173.7 (3)°, cis O–W–O angles are 89.8 (2)°, and W–O–C angles are 160.7 (4)°. $W(DIPP)_4$ is too crowded to react with a simple substrate such as an internal acetylene while $W(DMP)_4$ reacts with 3-hexyne to yield W(3-hexyne)$(DMP)_4$, with trimethylsilyl azide to yield $W(NSiMe_3)(DMP)_4$, with $(SiMe_3)CHN_2$ to yield $W[N_2CH(SiMe_3)](DMP)_4$, and with O_2, cyclohexene oxide, or iodosylbenzene to yield $W(O)(DMP)_4$. An attempt to replace the DMP ligands by S-2,4,6-$R_3C_6H_2$ (R = Me or *i*-Pr) ligands yielded $W(S)(DMP)_4$.

Introduction

The group 6 metals are some of the most interesting of the transition metals, in part because of the range of oxidation states that are available. During the last decade their chemistry has been developed extensively. However, molecules of the type MX_4, where X is an alkyl,[1-3] amide,[4] alkoxide,[5] or thiolate[6] group remain relatively scarce, particularly for Mo and W.[7] We have become especially interested in such species because we believe that di-

(1) Davidson, P. J.; Lappert, M. F.; Pearce, R. *Acc. Chem. Res.* **1974**, *7*, 209.
(2) Davidson, P. J.; Lappert, M. F.; Pearce, R. *Chem. Rev.* **1976**, *76*, 219.
(3) Schrock, R. R.; Parshall, G. W. *Chem. Rev.* **1976**, *76*, 243.
(4) Bradley, D. C.; Chisholm, M. H. *Acc. Chem. Res.* **1976**, *9*, 273.
(5) Bradley, D. C.; Mehrotra, R. C.; Gaur, D. P. *Metal Alkoxides*; Academic: New York, 1978.
(6) (a) Otsuka, S.; Kamata, M.; Hirotsu, K.; Higuchi, T. *J. Am. Chem. Soc.* **1981**, *103*, 3011. (b) Kamata, M.; Yoshida, T.; Otsuka, S.; Hirotsu, K.; Higuchi, T. *J. Am. Chem. Soc.* **1981**, *103*, 3572. (c) Roland, E.; Walborsky, E. C.; Dewan, J. C.; Schrock, R. R. *J. Am. Chem. Soc.* **1985**, *107*, 5795. (d) Listemann, M. L.; Dewan, J. C.; Schrock, R. R. *J. Am. Chem. Soc.* **1985**, *107*, 7207.

0020-1669/88/1327-0264$01.50/0